

Influence of EDTA/THPED Dual-Ligand on Copper Electroless Deposition

Lu Jianhong^{1,2}, Jimmy Yun^{2,3}, Lei Haiping¹, Tu Jiguo¹, Jiao Shu-qiang^{1,*}

¹ State Key Laboratory of Advanced Metallurgy, University of Science and Technology Beijing, Beijing 100083, China

² Changzhou Institutes of Advanced Materials, Beijing University of Chemical Technology, Changzhou 213164, China

³ School of Chemical and Pharmaceutical Engineering, Hebei University of Science and Technology, Shijiazhuang 050018, China

*E-mail: sjiao@ustb.edu.cn

Received: 26 January 2018 / Accepted: 2 March 2018 / Published: 10 May 2018

Single ligand electroless plating process has been studied extensively in the past decades, this study investigates the advantages of using a dual ligand system (EDTA/THPED) on electroless plating process. Electrochemistry techniques including mixed potential and linear sweep voltammetry (LSV) are used to examine the fundamental deposition mechanism of dual ligand system, providing critical information for dual ligand formulation design. Mixed potential tests indicated that increasing the Tetrakis (2-hydroxypropyl) ethylenediamine (THPED) concentration negatively shifts the electrode potential. The overall process was divided into three regions: induction, transition and stability. The degree of potential negatively shifted at each region was related to absorption, the type of redox reaction, ion diffusion and migration. Electrochemical analyses showed that there was an obvious peak for all anodic and cathodic reactions, respectively at around -0.42V and -0.57 V, whereby the current density depended on the THPED concentration. Moreover LSV study demonstrated control factor of autocatalytic reactions is cathodic reduction process of copper ion. The electroless deposition rate results were also in good agreement with mixed potential and electrochemical measurements, and the copper deposition rate increased significantly with the addition of THPED, and showed parabolic growth pattern. Metallographic studies of the dual-ligand electroless copper deposits revealed that their topographic structures had uniform and fine particle distribution, and a high-purity product without Cu₂O inclusions was detected. Copper layers displayed that the addition of THPED favored the formation of the preferred orientation on the (220) lattice plane.

Keywords: Electroless copper; Ligand; Mixed potential

1. INTRODUCTION

In 1947, Narcus first published a thesis on electroless copper plating [1], and the first commercial application of electroless copper plating was proposed by Cahill in 1957 [2]. Electroless copper is widely used in electronics, communications, mobile, machinery, aerospace, military, hardware etc. Ligands are one of the key components of the electroless copper process, which have an important influence on the copper lay grain properties, microstructure, reduction rate, energy consumption and stability [3-6]. Ethylenediaminetetraacetic (EDTA) is the most commonly used ligand in systems for electroless copper plating [7]. Other often used ligands are tartrate salt [8], citric salt [9], N-hydroxyethyl ethylene diamine triacetic salt (HEDTA) [10] and triethanolamine (TEA) [11]. Tetrakis (2-hydroxypropyl) ethylenediamine (THPED) is a novel ligand with special deposition properties [12].

The mechanism and method of electroless copper plating has been extensively studied, electrochemistry method is one of novel tools to research deposition process, including mixed potential method [13], linear sweep voltammetry or cyclic voltammetry (CV) method [14-15], electrochemical impedance spectroscopy (EIS) [16], electrochemical quartz crystal microgravimetry (EQCM) [17], differential electrochemical mass spectrometry (DEMS) [18], these studies were mainly focused on single ligand system, there were a few researches for dual or multi-ligand system can offer advantages with regards to deposition speed, stability and crystallization, which have recently become a hot research topic [19-22].

In this work, the deposition performances were systematically studied in electroless copper plating with a dual-ligand system using EDTA and THPED. The electrochemical features were analyzed by mixed potential and linear sweep voltammetry (LSV). The microstructure and composition of copper films were characterized by scanning electron microscopy (SEM), energy dispersive spectrometer (EDS), and X-ray diffraction (XRD), respectively.

2. EXPERIMENTAL

2.1 Materials and chemical

The chemicals used for this study included $\text{CuSO}_4 \cdot 5\text{H}_2\text{O}$, formaldehyde, EDTA, sodium hydroxide, PEG6000, 2,2'-Dipyridyl (from Aladdin Industrial Corporation) and Tetrakis (2-hydroxypropyl) ethylenediamine (from BASF Company).

The plating tests were performed on a pure copper piece (150 mm×100 mm×0.5 mm) in a 500ml glass beaker in a thermostatic water bath at a predetermined temperature. The pretreatment steps of the sample were given in our previous work^[4]: cleaning (ethanol) → rinsing (deionized water) → degreasing (5%NaOH) → rinsing (deionized water) → etching (1%HNO₃) → rinsing (deionized water) → drying & weighting → plating → rinsing (deionized water) → drying & weighting → characterizing. The electroless plating was carried out for 30 minutes at 30°C.

The ligand concentration in the plating solution was maintained at $0.06 \text{ mol}\cdot\text{L}^{-1}$ with a molar ratio of $[\text{total ligand}]/[\text{Cu}^{2+}]$ of 1.5. Table 1 lists the various experimental compositions tested in the dual-ligand bath.

Table 1. Chemical composition of the dual-ligand electroless copper system

Bath number	EDTA ($\text{mol}\cdot\text{L}^{-1}$)	THPED ($\text{mol}\cdot\text{L}^{-1}$)	Other items
1	0	0.06	CuSO ₄ ·5H ₂ O: $0.04 \text{ mol}\cdot\text{L}^{-1}$ NaOH: $0.2 \text{ mol}\cdot\text{L}^{-1}$ Formaldehyde: $0.13 \text{ mol}\cdot\text{L}^{-1}$ PEG 6000: $30 \text{ mg}\cdot\text{L}^{-1}$ 2,2'-dipyridyl: $6 \text{ mg}\cdot\text{L}^{-1}$
2	0.012	0.048	
3	0.024	0.036	
4	0.036	0.024	
5	0.048	0.012	
6	0.06	0	

2.2 Measure of deposition rate

The deposition rate was measured by the weight method, and is described by Equation (1).

$$v = \frac{10000 \Delta m}{\rho S t} \quad (1)$$

Where v is deposition rate, $\mu\text{m}\cdot\text{h}^{-1}$; Δm is the mass increment of the copper sample after plating, g; t is plating time, h; S is the area of copper substrate, cm^2 ; ρ is the copper density, $\text{g}\cdot\text{cm}^{-3}$.

2.3 Electrochemical analysis

Mixed potential and linear sweep voltammetry were carried out by the electrochemical workstation system (Shanghai CH Instruments, Inc, CHI660E) at room temperature. A conventional three-electrode cell was used with a pure copper rod as working electrode (WE) with an area of 1 cm^2 , inlaid into an epoxy resin, a Pt wire as counter electrode (CE) and a silver/silver chloride electrode as reference electrode (RE). For mixed potential measurements, the potential curve was recorded with respect to the open circuit potential (OCP). For LSV measurements, the scan rate of the anode curve was $2 \text{ mV}\cdot\text{s}^{-1}$ ranging between -200 mV to -600 mV in the absence of copper sulfate in electroless copper solution. The scan rate of the cathode curve was $2 \text{ mV}\cdot\text{s}^{-1}$ ranging between -400 mV to -1400 mV in the absence of formaldehyde in the electroless copper solution.

2.4 Characterization of the copper deposition layer

Scanning electron microscopy (SEM), energy dispersive spectrometer (EDX) and X-ray diffraction (XRD) were employed to characterize the structure and composition of the plating layer. A

Nova Nano SEM 450 (America FEI Company) was used to analyze the particle size distribution and compact degree of the deposition surface, meanwhile the EDX analysis confirmed the element composition of the copper coating. The phase structure of the surface layer was carried out by Cu-K α M21X X-ray diffraction (MAC Science Co. Ltd.). The voltage of the X-ray generator was set at 35 kv and the tube current was set at 30 mA. The scan range for the XRD was between 10° to 90°. The sampling width and scan speed were 0.02° and 8°·min⁻¹ respectively.

3. RESULTS AND DISCUSSION

3.1 Behaviors of mixed potential for different ligand solutions

Mixed potential theory has often been employed to study the electroless deposition process. According to the mixed potential mechanism, the mixed potential of an electroless plating solution was a thermodynamic factor and represented the reaction tendency. The electroless plating has been described to occur due to a combination of the oxidation and reduction partial faradaic process simultaneously at one electrode and determines the potential of one electrode, called the mixed potential (E_{mix}). This is the potential at which the same partial current and no-net current flows through the system [23-27]. Only when E_{mix} is more negative than the reduction potential of the metal complex ions in the plating solution, can the metal complexation ions be likely to be reduced to metal atoms. In other words, the tendency of the redox reaction becomes stronger as the mixed potential becomes more negative. Some studies have also confirmed that the deposition rate increases correspondingly when the mixing potential of the electroless copper plating system is negatively shifted [25].

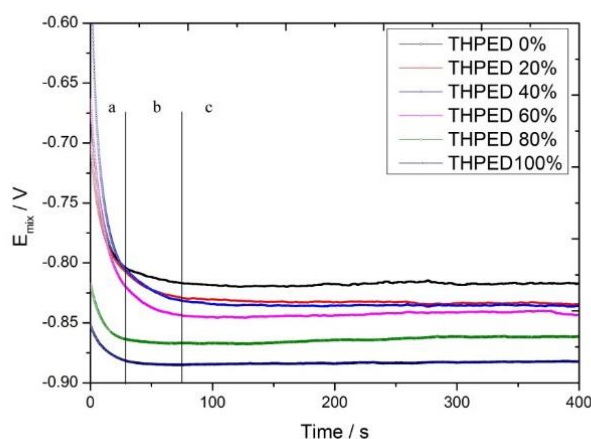


Figure 1. Mixed potential–time ($E_{\text{mix}}-t$) curves of the dual-ligand electroless solution on a copper electrode.

Fig. 1 and Table 2 show the mixed potential changes ($E_{\text{mix}}-t$) with different ligand systems during Cu electroless deposition at 23 ± 1 °C. For the different ligand systems (Samples 1-6 will be

used herein as stated in Table 1), the terminal mixed potential range was between -0.818V and -0.883V. The terminal mixed potential of sample 1 (containing 100% THPED) was -0.883V, while the potential of sample 6 (containing 0% THPED) was -0.818V. As seen from these results, the mixed potential was negatively shifted with the increase of THPED concentration.

Table 2. Mixed potential for different ligand systems

Bath number	Mixed potential (volt)
1	0.883
2	0.862
3	0.840
4	0.837
5	0.833
6	0.818

For the purpose of the following discussions, the overall deposition process was divided into three regions to describe the mixed potential change, the induction region (a region), transitional region (b region) and stable region (c region) as stated in Fig.1. For the induction region (a region), the potential falls off very fast within the first 35 seconds. This stage is the induction period, defined as the time necessary to reach the mixed potential [19]. It indicates that many electronegative ions and a small amount of electropositive ions are immediately adsorbed on the copper surface in those moments when the electrode was immersed into the electroless plating solution. This is because the diffusion-migration velocity of the electronegative ions (such as OH⁻) is relatively fast, while the diffusion-migration velocity of the electropositive ions (such as CuL²⁺) is slow, further leading to the potential fall off, as similarly described in the literature [7,13,28-30].

For the transitional region (b region), once a certain number of active ions are gathered on the catalytic surface, the redox reactions begin. The neutral formaldehyde is oxidized while the electropositive copper-ligand component and the electronegative OH⁻ are consumed at the same time. However, the difference in the diffusion-migration velocities of copper and OH⁻ ions leads to an excess of copper ions relative to OH⁻ at some potential. The adsorption processes continue until the saturation conditions are reached, and then the potential falls off slowly.

For the stable region (c region), the diffusion and migration of the electropositive copper ions quicken and are driven by the potential. The reactions become stable in this region as the supply rate of ions is gradually close to their consumption rate after 80 s, and finally the mixed potential remains unchanged.

3.2. Linear sweep voltammetry (LSV) studies

Fig. 2 and 3 show the effects of THPED concentration on the formaldehyde oxidation current and the cupric ion reduction current. Fig. 2 presents the LSV curves for cupric ion without formaldehyde. It can be seen that all the measured reduction potentials were approximately the same as the voltage peak at around -0.57 V. This indicates that the electrochemical processes of the cupric ions were similar as that containing the varied THPED concentration. Moreover, the reduction current density was sensitive to the THPED concentration. The maximum value ($0.118 \text{ mA}\cdot\text{cm}^{-2}$) of the cathodic reduction current density corresponded to the highest THPED (100%) concentration, while the minimum value ($0.054 \text{ mA}\cdot\text{cm}^{-2}$) was obtained for the lowest THPED concentration (0%). These electrochemical characters are somewhat in agreement with the researches [17,31-32].

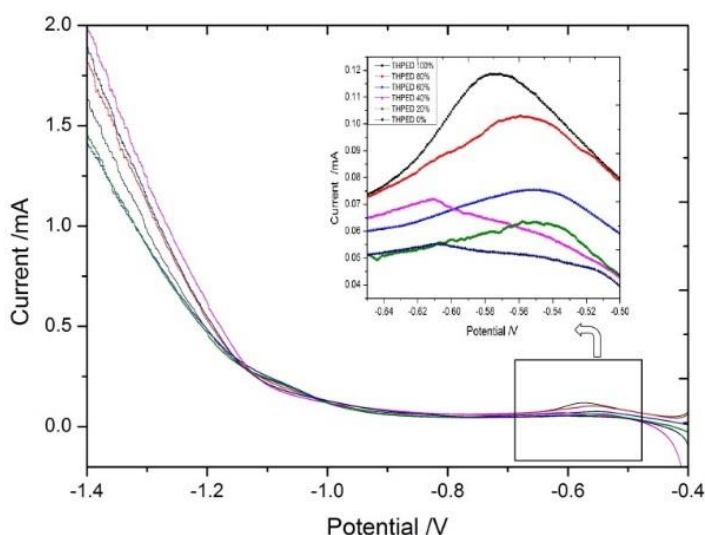


Figure 2. LSV curves of the cathodic reduction of Cu (II) ion in dual-ligand solution

Analogously, the oxidation of formaldehyde also displayed those properties. Fig. 3 shows the LSV curves for the oxidation of formaldehyde without cupric ion. It can be seen that there was an obvious oxidation peak at around -0.42 V. Similar to the Cu (II) reduction, the oxidation current density was related to THPED concentration. The maximum value of anodic oxidation current density was $0.770 \text{ mA}\cdot\text{cm}^{-2}$ at the highest THPED concentration, while the minimum value of $0.392 \text{ mA}\cdot\text{cm}^{-2}$ was obtained at the lowest THPED concentration. By comparing the reduction and oxidation current density, the reduction current (from 0.054 to $0.118 \text{ mA}\cdot\text{cm}^{-2}$) is one order of magnitude lower than the oxidation current (from 0.392 to $0.770 \text{ mA}\cdot\text{cm}^{-2}$), indicating the control factor of the above reaction system is cathodic reduction reaction of copper ion.

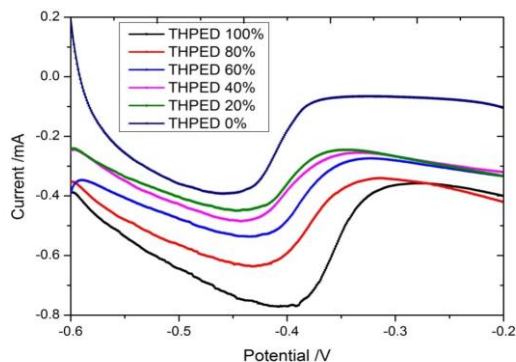


Figure 3. LSV curves of the anodic oxidation of formaldehyde in dual-ligand solution

Interestingly, the stability constant of the Cu(II)-THPED ligand (29.1) was higher than the stability constant of the EDTA ligand (18.0) [33]. The difference in stability constants was very large, meaning that the Cu(II)-THPED ligand would be difficult to dissociate free Cu^{2+} . Hence the current density of the Cu(II)-THPED plating system would be lower than that using EDTA. However, during the reduction of Cu(II), the current density of Cu(II)-THPED was higher than that of Cu(II)-EDTA. This phenomenon was explained by Paunovic [13] as the fact that the rate of dissociation of a complex is controlled by steric hindrance, which is concerned with donor atoms (such as O and N) and substituents (such as CH_2COOH and $\text{CH}_2\text{CH}[\text{OH}]\text{CH}_3$). Steric hindrance increases in the following order: tartrate, EDTA, THPED, CDTA, therefore, the dissociation rate constant (K_d) also increases in that order. As the dissociation rate of a ligand increases, the concentration of free $[\text{Cu}^{2+}]$ increases, and the current density also increases correspondingly.

3.3 Influence of different ligand ratios on deposition rate

Fig. 4 shows dependence of deposition rate on ligand ratio in an electroless copper solution. The deposition rate in pure EDTA ligand is $0.47 \mu\text{m}\cdot\text{h}^{-1}$, while the rate reaches $11.7 \mu\text{m}\cdot\text{h}^{-1}$ in a pure THPED ligand. This is approximately a 25 fold difference between the two ligand systems. And the rate dependence almost appears as a parabolic growth with the increase of THPED ligand concentration, and can be described by Equation (2).

$$V = 0.447 + 0.0276 \cdot \text{Con}_{(\text{THPED})} + 0.0008504 \cdot \text{Con}_{(\text{THPED})}^2 \quad (2)$$

These results are in agreement with the previously described results for mixed potential and linear sweep voltammetry. Chemical potential is the most essential factor that determines the direction of a chemical reaction and is the driving force of a chemical reaction. The mixed potential negatively shifts with increasing THPED concentration, provides that driving force to reduce copper ions in an electroless solution. On the other hand, from the linear sweep voltammetry test data, the current densities of both reactions increase with increasing THPED concentration, similarly provide a foundation for the dynamics of the deposition rate increase.

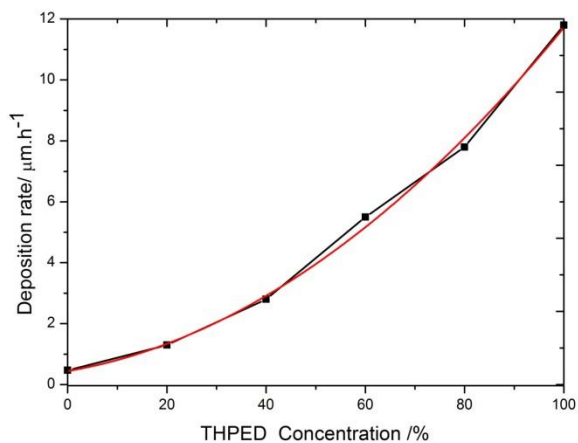


Figure 4. Dependence of deposition rate on ligand ratio in an electroless copper solution (red line is the fitted parabolic curve)

3.4 Surface coating microstructure

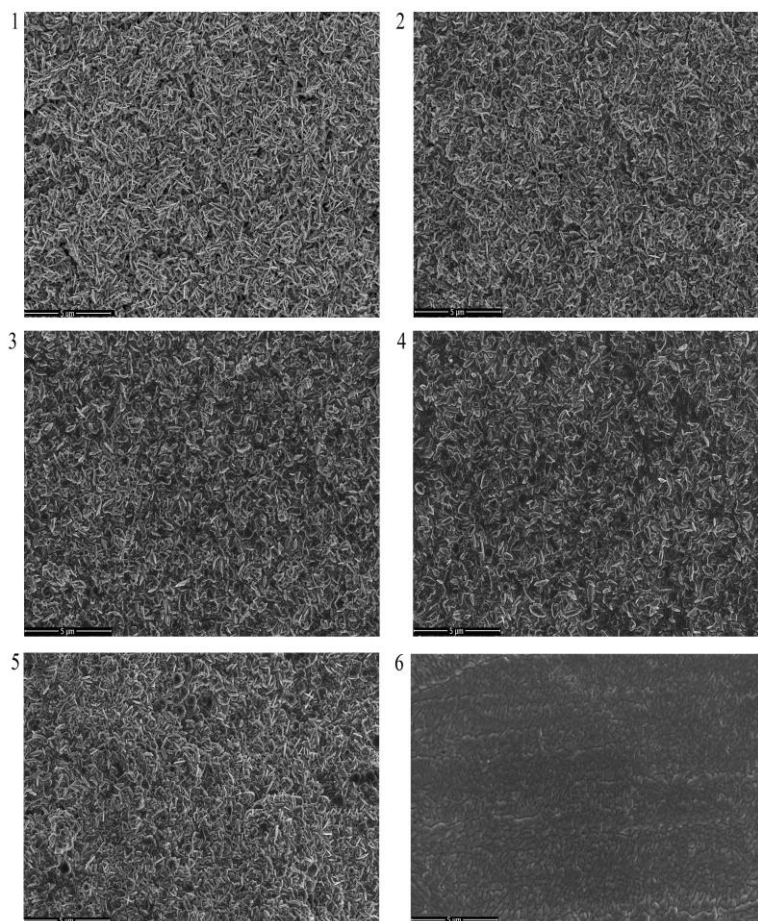


Figure 5. SEM images of copper layers obtained in baths: samples 1, 2, 3, 4, 5 and 6 (as described in Table 1).

Fig. 5 displays SEM images of the copper layers obtained using different ligand concentrations after plating for 30 minutes. As can be seen, when using a 100% THPED bath (sample 1), the obtained grains appeared pine needle shaped with a needle length of 0.5-1.0 μm . This is possibly due to the fast reaction rate of the pure THPED system, as there is not enough time for reaction bubbles to escape from the inner Cu seeds and partly blocks the metal formation. On the other hand, bubbles on the outer fresh surface is relatively easy to escape and deposition particles preferentially grow outward. With an increase in EDTA concentration, reaction rate slows gradually, and the bubble escape rate on each direction tends to balance off. As a result, the surface morphology appeared granulous when the grain size became smaller and smaller.

The grain size ranged between 0.2 μm and 0.8 μm . To study the coating composition of the deposition layers in more detail, EDX analysis was performed (Fig. 6). The EDX gives the evidence for the presence of only Cu for all the formed layers. There were no other impurity elements detected.

Fig. 7 presents the XRD patterns of the electroless copper plating samples. Diffraction peaks can be observed at $43.3^\circ \pm 0.1^\circ$, $50.48^\circ \pm 0.1^\circ$, $74.1^\circ \pm 0.1^\circ$, corresponding to Cu (111), (200) and (220) [34], and (220) lattice plane is main component. Therefore all deposited Cu layers had a face centered cubic (FCC) structure. The copper oxide phase was not detected in the coating, confirming that the coated copper was highly pure with all ligand compositions in the plating bath.

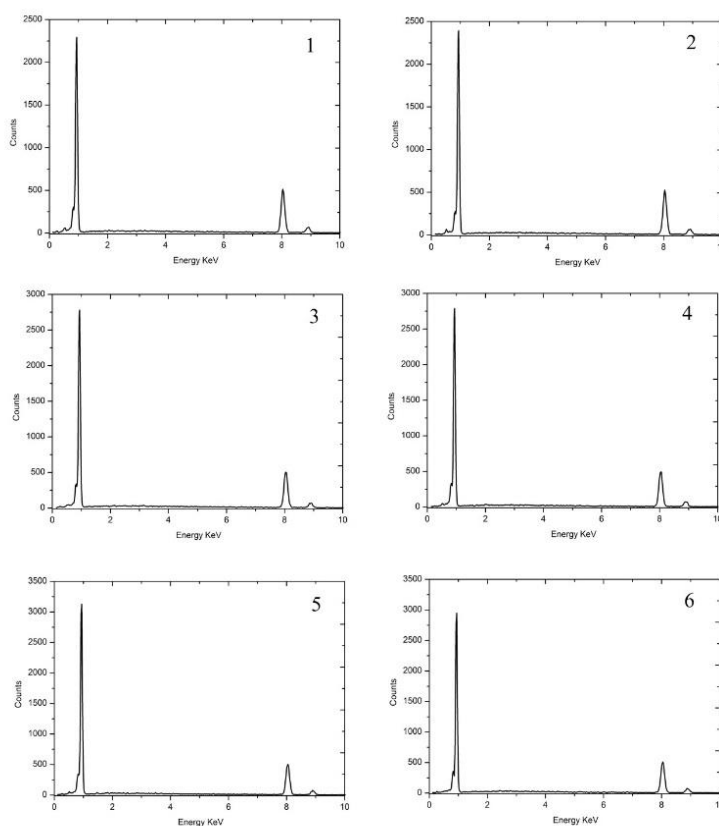


Figure 6. EDX spectrograms of copper layers obtained in baths 1, 2, 3, 4, 5 and 6 (as described in Table 1).

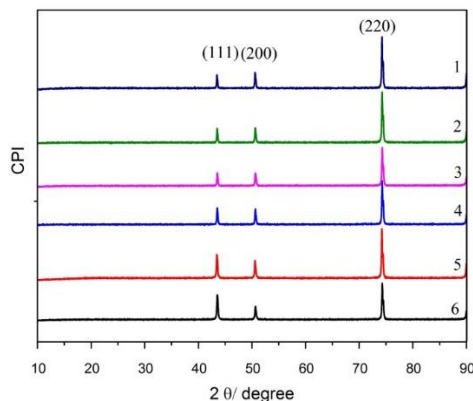


Figure 7. XRD patterns of electroless copper layers obtained using different ligand ratios in the plating bath.

Table 3. The relative intensity and ratio of XRD peaks of copper layers obtained using different ligand concentrations

Sample number	peak height			I_{220}/I_{111}
	(111)	(200)	(220)	
1	926	1052	2972	3.21
2	957	972	2906	3.03
3	863	856	2218	2.57
4	1090	1017	2539	2.33
5	1485	1159	2863	1.93
6	1515	898	2132	1.41

Table 3 summarizes the relative intensity (peak height) and the ratio of XRD peaks of copper layers obtained using the different ligand ratios. For the (200) lattice plane, there was no observable variation for the different samples, while the intensity ratio of I_{220}/I_{111} changed from 1.41 to 3.21 as the THPED concentration increased from 0% to 100%. These results show that an increase in THPED concentration leads to a tendency for the formation of the preferred orientation on the (220) lattice plane.

4. CONCLUSIONS

In this work, the effects of different ligand systems on the plating process were studied in detail. It was found that increasing the THPED concentration of the solution made the mixed potential negatively shift. Electrochemical measurements showed that there was an obvious peak for all anodic and cathodic reactions, at approximately -0.42 V and -0.57 V, respectively. The current density was

sensitive to THPED concentration, showing the trend that the higher the THPED concentration is, the greater the current density is. The electroless deposition rate results were in good agreement with mixed potential and electrochemical measurements. And the deposition rate increased significantly with THPED addition, with a parabolic dependence. LSV data indicates that the control factor of these autocatalytic reactions is cathodic reduction reaction of copper ion. The topographic structures of the dual-ligand electroless copper deposits showed a uniform and fine particle distribution. The X-ray diffraction results of the electroless copper layers verified that the addition of THPED favored the formation of the preferred orientation on the (220) lattice plane.

ACKNOWLEDGEMENT

This work was sponsored by the Jiangsu Innovative & Entrepreneurial Programme.

References

1. H. Narcus, *Metal Finishing*, 45(1947)964.
2. Farid Hanna, Z. Abdel Hamid, A. Abdel Aal, *Mater. Lett.*, 58 (2003)104.
3. Y. Shacham-Diamand, T. Osaka, Y. Okinaka, A. Sugiyama, V. Dubin, *Microelectron. Eng.*, 132(2015)35.
4. J.H. Lu, H.D. Jiao, S.Q. Jiao, *Chinese J. Eng.*, 39(2017)1380.
5. S. Shingubara, Z.L. Wang, O. Yaegashi, R. Obata, H. Sakaue, T. Takahagi, *Electrochem. Solid. St.*, 7(2004)C78.
6. S. Miura, H. Honma, *Surf. Coat. Tech.*, 169-170 (2003)91.
7. E. Norkus, V. Kepenienė, A. Vaškėlis, J. Jačiauskienė, I. Stalnionienė, G. Stalnionis, *Chemija*, 17(2006)20.
8. S. Shukla, S. Seal, J. Akesson, R. Oder, R. Carter, Z. Rahman, *Appl. Surf. Sci.*, 182(2001)35.
9. B. Yang, F.Z. Yang, L. Huang, S.K. Xu, G.H. Yao, S.M. Zhou, *J. Electrochem.*, 13(2007)425.
10. J. Li, P.A. Kohl, *J. Electrochem. Soc.*, 150(2003)558.
11. W.H. Lin, H.F. Chang, *Surf. Coat. Tech.*, 107 (1998)48.
12. Y.J. Zheng, W.H. Zou, D.Q. Yi, Z.Q. Gong, X.H. Li, *J. Cent. South. Univ. Tech.*, 12(2005)82.
13. M. Paunovic, *J. Electrochem. Soc.*, 124(1977)349.
14. Y.M. Lin, S.C. Yen, *Appl. Surf. Sci.*, 2001 (178)116.
15. Y. Liao, S.T. Zhang, R. Dryfe, *Particuology*, 10(2012)487.
16. T. Anik, A. E.L. Haloui, M. Ebn Touhami, R. Tourir, H. Larhzil, M. Sfaira, M. Mcharfi, *Surf. Coat. Tech.*, 245(2014)22.
17. Z. Jusys, R. Pauliukaite, A. Vaskelis, *Phys. Chem. Chem. Phys.*, 1(1999)313.
18. A. Vaskelis, Z. Jusys, *Analytica Chimica Acta.*, 305(1995)227.
19. M.Z. An, Z.M. Tu, J.S. Zhang, Z.L. Yang, Z.N. Huang, *Electroplat. Poll. Contrl.*, 10(1990)1.
20. Y.J. Zheng, C.H. Li, W.H. Zou, *Mater. Rev.*, 20(2006)159.
21. W.M. Zeng, C.S. Wu, Y.S. Wu, *J. Mater. Prot.*, 34(2001)24.
22. X. Gu, Z.C. Wang, C.J. Lin, *Electrochem.*, 10(2004)14.
23. E. Norkus, A. Vaskelis, J. Jaciauskiene, J. Vaiciuniene, E. Gaidamauskas, D.L. Macalady, *J. Appl. Electrochem.*, 35(2005)41.
24. K.G. Mishra, R.K. Paramguru, *Metall. Mater. Trans. B*, 30(1999)223.
25. C.H. Lee, S.C. Lee, J.J. Kim, *Electrochim. Acta.*, 50(2005)3563.
26. J. Li, P.A. Kohl, *Plat. Surf. Finish.*, 91(2004)2.
27. P. Bindra, *J. Appl. Electrochem.*, 17(1987)1254.

28. X. Gu, G.H. Hu, Z.C. Wang, C.J. Lin, *Acta. Phys. Chim. Sina.*, 20(2004)113.
29. M. Ramasubramanian, B.N. Popov, R.E. White, K.S. Chen, *J. Electrochem. Soc.*, 146(1999)111.
30. R. Pauliukaite, G. Stalnionis, Z. Jusys, A. Vaskelis, *J. Appl. Electrochem.*, 36(2006)1261.
31. A. Vaskelis, J. Jaciauskiene, I. Stalnioniene, E. Norkus, *J. Electroanal. Chem.*, 600(2007)6.
32. Z. Jusys, G. Stalnionis, E. Juzeliunas, A. Vaskelis, *Electrochim. Acta.*, 43(1998)301.
33. J.H. Lu, H.D. Jiao, S.Q. Jiao, *Electroplat. Finish.*, 13(2016)705.
34. F.T. Hu, S. Yang, H.Z. Wang, M. Li, *J. Electron. Mater.*, 44(2015)4516.

© 2018 The Authors. Published by ESG (www.electrochemsci.org). This article is an open access article distributed under the terms and conditions of the Creative Commons Attribution license (<http://creativecommons.org/licenses/by/4.0/>).